Surface Science 679 (2019) 17–23

Contents lists available at ScienceDirect

Surface Science

journal homepage: www.elsevier.com/locate/susc

(0001) Interfaces between M_2O_3 corundum oxides (M = Al, Ti, V, Cr, Fe).

H.-L.T. Le, J. Goniakowski, C. Noguera*

CNRS-Sorbonne Université, UMR 7588, INSP, Paris F-75005, France

ARTICLE INFO

Keywords:
Transition metal corundum oxides
Oxide/oxide interfaces
DFT + U calculations
Interfacial redox reaction
Band off-sets
Ionicity

ABSTRACT

The structural quality of oxide/oxide interfaces, their chemistry, and the nature of their electronic states are critical properties for new promising applications and require continuous advances in their fundamental understanding. To this goal, we have performed a theoretical study of a series of (0001) M_2O_3/M'_2O_3 interfaces (M, M' = Al, Ti, V, Cr, Fe) between simple and transition metal oxides crystallizing in the corundum structure. Our DFT + U results reveal two qualitatively different mechanisms of interface charge redistribution: an interfacial oxidation–reduction reaction occurring at Ti_2O_3/V_2O_3 and Ti_2O_3/Fe_2O_3 contacts, and a much weaker electron transfer along anion-cation bonds which follows the difference of ionicity between the two constituting oxides at all interfaces. At variance with interfaces between *sp* semiconductors, the band bending does not propagate beyond one or two atomic layers. More generally, our results show that the nature of the interface electronic structure and the energetics of its formation can be tightly linked to the properties of the corresponding bulk oxides, thus providing a precious tool for designing oxide/oxide interfaces of required characteristics.

1. Introduction

Oxides have long been used in a variety of applications, including catalysis, electronics and optoelectronics, or as thermal or electrical insulating barriers. More recently, all-oxide electronic devices have progressively replaced many of those traditionally based on semiconductors. In these fields, the structural quality of oxide/oxide interfaces, their precise composition, and the nature of their electronic states play a decisive role. It is also worth mentioning a more fundamental interest in oxide interfaces triggered by the discovery of emergent phenomena associating charge, spin and orbital degrees of freedom [1].

Despite this wide context, there are very few systematic studies of oxide/oxide interfaces which try to relate their characteristics to those of the constituting oxides. The most significant ones concern perovskite oxides [2] or the Cr_2O_3/Fe_2O_3 interface [3–6]. Here our goal was to perform a thorough and systematic study of six (0001) interfaces between transition metal corundum oxides, including Ti_2O_3, V_2O_3, Cr_2O_3 and Fe_2O_3. We have also considered an hypothetical Ti_2O_3/Al_2O_3 interface as to include a more ionic oxide with pure *sp* character. Using a DFT + U approach, we have analyzed the nature of the states close to the Fermi level, the interface charge transfers, and the formation of interfacial dipoles. We link these interface characteristics to the band alignment between the constituting oxides and their difference in ionicity. Moreover, we evidence strong similarities between the energetics of M_2O_3/M'_2O_3 interfaces and the formation energies of mixed $MM'O_3$ oxides of corundum-type structures.

The paper is organized in the following way. After a section describing the computational methods and settings (Section 2), we summarize the results on anionic-type and cationic-type interfaces (Section 3). A discussion (Section 4) highlights two qualitatively different mechanisms of interface charge redistribution, both characterized by extremely short penetration lengths, and establishes a direct link between the interface stability and the tendency for cationic mixing in the corresponding bulk corundum-type oxides. A conclusion follows (Section 5).

2. Computational details

DFT calculations are performed with the Vienna Ab-initio Simulation Package (VASP) [7,8] using the Projector Augmented Wave (PAW) method [9,10] to represent the electron-core interaction and a 400 eV energy cutoff in the development of Kohn–Sham orbitals on a plane-wave basis set. Transition metal 3*p* states are systematically considered as semi-core states. The DFT + U approach proposed by Dudarev [11,12] is used together with the dispersion-corrected exchange-correlation functional (optB88-vdW) [13–15], as to improve the description of interfacial electronic structure and energetics. As in our previous work [16], we use *U* values equal to 1.0, 1.7, 3.0, and 3.0 for Ti_2O_3, V_2O_3, Cr_2O_3, and Fe_2O_3, respectively, which correctly account for the electronic characteristics of the bulk oxides. All calculations are

---

* Corresponding author.
E-mail address: claudine.noguera@insp.jussieu.fr (C. Noguera).

https://doi.org/10.1016/j.susc.2018.08.015
Received 29 June 2018; Received in revised form 22 August 2018; Accepted 23 August 2018

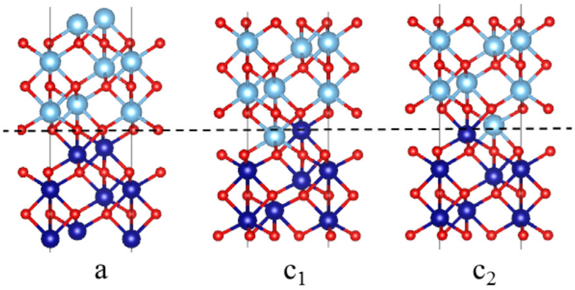

Fig. 1. Atomic structure at anionic (a) and cationic (c_1 and c_2) interfaces. Oxygen and metal atoms are represented with red and blue (dark or light) balls, respectively. (For interpretation of the references to color in this figure legend, the reader is referred to the web version of this article.)

Table 1
Characteristics of constituting bulk M_2O_3 and M'_2O_3 oxides (at average in-plane lattice parameter) and of the most stable cationic (c_1 or c_2) and anionic (a) M_2O_3/M'_2O_3 interfaces: Bader charges of cations Q_M and oxygen atoms Q_O (e), cation magnetic moments μ_M (μ_B). Total Bader charges Q_{int} of each side of the interface (e) and interface energies E_{int} (J/m^2).

	Ti_2O_3	Al_2O_3	Ti_2O_3/Al_2O_3 (c_1)	Ti_2O_3/Al_2O_3 (a)
Q_M	1.90	2.49	1.84, 1.98/2.50	1.97, 1.93/2.50
μ_M	0.0	0.0	0.0,0.0/0.0	0.0/0.0
Q_O	−1.27	−1.66	−1.39/−1.56	−1.48
Q_{int}	–	–	−0.33/+0.33	−0.29/+0.29
E_{int}	–	–	0.25	0.27
	Ti_2O_3	V_2O_3	Ti_2O_3/V_2O_3 (c_1)	Ti_2O_3/V_2O_3 (a)
Q_M	1.91	1.84	2.02, 2.10/1.62,1.72	2.01, 2.02 / 1.75, 1.86
μ_M	0.0	1.8	0.3, 0.0/2.3,2.1	0.3, 0.1 / 2.0, 2.0
Q_O	−1.27	−1.23	−1.26/−1.24	−1.28
Q_{int}	–	–	+0.44/−0.44	+0.27 / −0.27
E_{int}	–	–	−0.28	−0.18
	Ti_2O_3	Cr_2O_3	Ti_2O_3/Cr_2O_3 (c_1)	Ti_2O_3/Cr_2O_3 (a)
Q_M	1.91	1.77	2.01/1.69	1.96 / 1.73, 1.77
μ_M	0.0	2.9	0.4/3.0	0.7, 0.5 / 3.0, 2.8
Q_O	−1.27	−1.18	−1.25/−1.21	−1.24
Q_{int}	M	–	+0.20/−0.20	+0.14/−0.14
E_{int}	–	–	0.15	0.10
	Ti_2O_3	Fe_2O_3	Ti_2O_3/Fe_2O_3 (c_2)	Ti_2O_3/Fe_2O_3 (a)
Q_M	1.92	1.74	2.03,2.15 / 1.44, 1.49	2.08, 2.05 / 1.66, 1.50
μ_M	0.0	4.1	0.1 / 3.7	0.2, 0.1 / 3.9, 3.7
Q_O	−1.28	−1.16	−1.23/−1.18	−1.21
Q_{int}	–	–	+0.68/−0.68	+0.47/−0.47
E_{int}	–	–	−0.65	−0.45
	V_2O_3	Cr_2O_3	V_2O_3/Cr_2O_3 (c_1)	V_2O_3/Cr_2O_3 (a)
Q_M	1.84	1.77	1.86 / 1.76	1.86, 1.87 / 1.77, 1.77
μ_M	1.7	2.9	1.8 / 2.8	1.7, 1.8 / 2.9
Q_O	−1.22	-1.18	−1.22 /−1.20	−1.21
Q_{int}	–	–	+0.08/-0.08	+0.06/−0.06
E_{int}	–	–	0.02	0.01
	V_2O_3	Fe_2O_3	V_2O_3/Fe_2O_3 (c_2)	V_2O_3/Fe_2O_3 (a)
Q_M	1.85	1.74	1.96 /1.66	1.90, 1.84 / 1.76, 1.74
μ_M	1.7	4.1	1.5 / 4.0	1.6, 1.8 / 4.1, 4.1
Q_O	-1.23	-1.16	-1.22/-1.19	-1.21
Q_{int}	-	-	+0.15/-0.15	+0.08/-0.08
E_{int}	-	-	0.10	0.13
	Cr_2O_3	Fe_2O_3	Cr_2O_3/Fe_2O_3 (c_2)	Cr_2O_3/Fe_2O_3 (a)
Q_M	1.77	1.74	1.79 / 1.76	1.79, 1.77 / 1.78, 1.76
μ_M	2.9	4.1	2.9 /4.1	2.8, 2.9 / 4.1, 4.1
Q_O	-1.18	-1.16	-1.18 /-1.18	-1.19/-1.17
Q_{int}	-	-	+0.02/-0.02	-0.00/+0.00
E_{int}	-	-	0.12	0.16

spin-polarized and the non-magnetic (NM for Al_2O_3 and Ti_2O_3), G-type (for Cr_2O_3 and V_2O_3) and C-type (for Fe_2O_3) antiferromagnetic (AF) ground state orderings computed for the corresponding bulk materials [16] are systematically preserved. Ionic charges are estimated with the partition scheme proposed by Bader [17,18] and magnetic moments are obtained by integration of the spin density within the Bader's volumes. Bulk and interface configurations are plotted with VESTA [19].

Three types of interfaces are considered, involving either an interfacial oxygen layer (Fig. 1, left, labeled *a* or *anionic* in the following), or an interfacial cationic bi-layer (Fig. 1, right, labeled c_1 and c_2 or *cationic*). At *a* interfaces, the interfacial atoms are all equivalent, with two cation first neighbors of one type and two of the other. On each side of this layer, the two cations are nonequivalent. One is linked via a short inter-plane bond to a cation of its own type ("bulk-like" bond) and one with a cation of opposite type ("interfacial" bond). At *c* interfaces, a cation of a given type may occupy two inequivalent positions. In the configuration c_1, an interfacial cation has three in-plane first neighbors, zero inter-plane first neighbor and six inter-plane second neighbors with cations of opposite type. In the second configuration (noted c_2) in which the two interfacial cations have exchange positions, an interfacial cation has three in-plane first neighbors, one inter-plane first neighbor and three inter-plane second neighbors with cations of opposite type. In both cases, the oxygen atoms which are the closest to the interface have three cations first neighbor of one type and one of the other type, instead of having four cations first neighbors of the same type in the bulk. It should be noted that all anionic and cationic interfaces are non-polar [20]. Indeed, their repeat units of respective composition $O_{1.5}/M_2/O_{1.5}$ (for the anionic interface) and $M/O_3/M$ (for the cationic interfaces) bear no dipole moment and thus do not produce a polarization discontinuity [21].

Interfaces are represented by superlattices with six M_2O_3 formula units of each oxide, with an interface registry which preserves the corundum stacking. We have checked that alternative registries produce less stable configurations. The in-plane lattice parameters are fixed at the average values between those of the two corresponding bulks (4.80 Å, 5.14 Å, 5.05 Å, 5.04 Å, 5.06 Å, for bulk Al_2O_3, Ti_2O_3, V_2O_3, Cr_2O_3, and Fe_2O_3, respectively [16]), and the out-of-plane parameters are optimized until the corresponding components of stress tensor are smaller than 0.01 eV Å^{-3}. In addition, all atomic position are relaxed until maximum forces get smaller than 0.01 eV Å^{-1}. The Brillouin zone of the (1 × 1) interface unit cell is sampled on a Γ-centered (8 × 8 × 1) Monkhorst–Pack grid [22].

The stability of an M_2O_3/M'_2O_3 interface is estimated from the interface energy E_{int}:

$$E_{int} = \frac{(E_{M_2O_3/M'_2O_3} - (E'_{M_2O_3} + E'_{M'_2O_3}))}{2S} \tag{1}$$

in which $E_{M_2O_3}$, $E_{M'_2O_3}$ are the energies of six formula units of bulk M_2O_3 and M'_2O_3 materials (at the average in-plane lattice parameter), $E_{M_2O_3/M'_2O_3}$ is the energy of the constituted heterostructure, and S is the interface area. Factor 2 accounts for the two equivalent interfaces in the unit cell.

3. Results

In this section, the numerical results for the anionic and cationic interface structures are reported. We start by a comprehensive description of the cationic interfaces, and, in a second step, we highlight their similarities and differences with the anionic interfaces.

3.1. Cationic interfaces

Table 1summarizes the electronic, magnetic and energetic properties of the most stable cationic configurations for all interfaces under consideration. Figs. 2 and 3 display their local density of states (LDOS) projected on the cations at the interface and in bulk-like positions.

All interfaces are subject to similarly weak structural distortions since the lattice mismatch between the constituent oxides never exceeds 1.5%, except between Ti_2O_3 and Al_2O_3 for which it reaches 7%. At variance, the interface electronic structures display much bigger differences with respect to their bulk counterparts. On the one hand, at the Ti_2O_3/V_2O_3 and Ti_2O_3/Fe_2O_3 interfaces, a strong charge redistribution